UNIVERSITY OF CALIFORNIA SAN DIEGO

RNAs Regulate TOP1 Protein Interactome

A Thesis submitted in partial satisfaction of
the requirements for the degree Master of Science

in

Biology

by

Paola Orozco

Committee in charge:

Professor Shannon Lauberth, Chair
Professor James T. Kadonaga
Professor Amy Pasquinelli

2020

The Thesis of Paola Orozco is approved, and it is acceptable in quality and form for publication on microfilm and electronically:

_____

_____

_____
Chair

University of California San Diego

2020

DEDICATION

First, I dedicate with love this work to my parents Rafael Orozco and Lusmila Talamantes for being my number one supporters and for their continuous guidance. For teaching me the value of perseverance and to never give up on my dreams.

To Hareth Abdalkarim, for his unconditional friendship, support and words of encouragement.

To Homa Rahnamoun, not only for training me and for her continuous scientific support throughout this journey, but also for building a long-lasting friendship with me.

To Dr. Don Helinski, for making my days in the lab so special with his kind words and for his continuous advice.

With a lot of gratitude, I dedicate this work to my mentor Dr. Shannon Lauberth for believing in me and for inspiring me to always think big and work hard to achieve my goals.

TABLE OF CONTENTS

LIST OF FIGURES

LIST OF TABLES

ACKNOWLEDGEMENTS

I would like to acknowledge Lidija Vukovic and Anup Mazumder for their incredible work and help during the COVID19 pandemic because without their help this work would not have been possible.

I would also like to acknowledge Vincent Aguilar for working with me and for his remarkable patience.

This paper is coauthored with Rahnamoun, Homa. The thesis author was the primary author of this paper.

ABSTRACT OF THE THESIS

RNAs Regulate TOP1 Protein Interactome

by

Paola Orozco

Master of Science in Biology

University of California San Diego, 2020

Professor Shannon Lauberth, Chair

Human Topoisomerase 1 (TOP1) is a dynamic enzyme that functions to overcome topological constraints on the DNA that are caused by strand separation. In this study, we demonstrate that TOP1 is an RNA binding protein (RBP) as revealed by ultraviolet-crosslinked RNA immunoprecipitation (UV-RIP) analyses at intergenic and promoter regions in colon cancer cells treated with acute doses of tumor necrosis alpha (TNF-α). Through biochemical methods, we found that TOP1 directly interacts with different RNAs. Furthermore, proteomic analyses reveal that RNAs add an additional layer of regulation by contributing to the maintenance of TOP1 ribonucleoprotein complexes.

Introduction

DNA topoisomerase I (TOP1) modulates essential cellular processes such as DNA replication, transcription, and chromatin remodeling by removing topological constraints of the DNA double helix that can otherwise inhibit these processes[1-4]. Rapid unwinding of the DNA strands during these cellular responses leads to substantial torsional stress that may hinder gene expression by causing the formation of RNA-DNA hybrids known as R-loops and double-stranded DNA breaks (DSBs)[1, 5-8]. TOP1 resolves torsional stress by introducing a transient single-strand nick on the DNA through its catalytic intermediate known as the TOP1 cleavable complex (TOP1cc) followed by the rotation of the TOP1-bound DNA strand about the unbroken strand and the resealing of the nick[9]. Treatment with TOP1 poisons such as camptothecin (CPT) and its derivatives stabilizes the TOP1cc intermediate, that in turn leads to R-loop accumulation and DSB formation that results in the inhibition of gene expression (reviewed in [10]).

TOP1 is a crucial enzyme that is predominantly found in the nucleolus[11] and mediates various cellular processes within this nuclear subcompartment. TOP1 is essential in regulating the highly transcribed ribosomal genes[11-14]. TOP1 not only interacts with RNA Polymerase I (RNAPI), but also colocalizes with it at the nucleolar fibrillar centers where rDNA transcription takes place[15, 16]. Evidence in yeast demonstrated that loss of TOP1 leads to transcriptional blocks at ribosomal DNA (rDNA) repeats resulting in truncated transcripts[17]. Moreover, a recent study in HeLa cells identified TOP1 as an important pre-ribosomal RNA processing factor in the nucleolus[18]. TOP1 was further identified as a component of the Nop56p-associated pre-ribosomal complex which regulates pre-rRNA maturation. Interestingly, TOP1 also plays an important role in maintaining the morphology of the nucleolus as revealed by a decrease in the nucleolar size and the

displacement of crucial nucleolar factors such as NPM1 into the nucleoplasm upon TOP1 depletion[19].

Notably, TOP1 also plays important enzymatic roles during transcription events within the nucleoplasm. Early *in vitro* studies demonstrated that TOP1 is a cofactor for activator-dependent transcription by RNA Polymerase II (RNAPII) and it facilitates the assembly of the TFIID-TFIIA complex to promote transcription initiation[20, 21]. In accordance with this, a recent study reported that TOP1 relaxation activity is crucial in modulating DNA supercoiling to support transcription initiation and RNA Polymerase II (RNAPII) pause-release[22]. More specifically, TOP1 activity is mostly inactivated at transcription start sites to maintain negative supercoiling required for promoter melting[22]. TOP1 is then stimulated through its interactions with the BRD4-phosphorylated C-terminal domain of RNAPII to resolve torsional stress and promote pause-release[22]. Additionally, TOP1 has been shown to be essential in the regulation of transcription at androgen receptor and Aire-regulated super-enhancers in prostate cancer and medullary thymic epithelial cells, respectively[23, 24].

The subnuclear localization of TOP1 is highly dynamic. In a normal cellular context, TOP1 is a mobile enzyme that is in constant efflux between the nucleoplasm and nucleolus with its mobility being slower in the latter[25]. However, its localization is sensitive to various cellular conditions. Inhibition of RNA synthesis, in particular ribosomal RNA (rRNA) synthesis, shifts TOP1 from being primarily located in the nucleolus to become more evenly spread throughout the nucleus[11, 13, 26]. Furthermore, cellular stress induced by CPT treatment results in TOP1 redistribution from the nucleolus to the nucleoplasm presumably by inducing TOP1 SUMOylation and by disrupting RNA synthesis[25, 27-29].

In addition to the subnuclear localization of TOP1, its enzymatic activity is tightly controlled through different mechanisms due to the critical roles of TOP1 at actively transcribed genomic loci. TOP1 relaxation activity has been shown to be stimulated through its interactions with important transcription regulators such as p53, ARF and NKX3.1[30-32]. On the other hand, TOP1 activity was reported to be attenuated through interactions with the tumor suppressor PAR-4 which sequesters TOP1 from the DNA to prevent TOP1-induced genomic instability[33]. Moreover, post-translational modifications of TOP1 also play a crucial role in its regulation. Namely, SUMOylation of TOP1 at highly transcribed regions assists in the recruitment of splicing factors to prevent R-loop accumulation and DSBs[34].

While several mechanisms underlying the regulation of TOP1 at actively transcribed regions have been explored, the reciprocal roles of RNAs in regulating TOP1 remain unknown. Interestingly, many DNA-binding proteins have been shown to exhibit RNA binding capabilities[35, 36]. In line with this, a few recent studies have identified TOP1 to be among noncanonical mRNA binding factors through unbiased approaches[37-39]. In addition, the long non-coding RNA (lncRNA) *NORAD* was found to control the ability of RBMX to assemble a TOP1-containing ribonucleoprotein complex that is essential for maintaining genomic stability[40]. Consistent with these findings, TOP1 was also recently identified to be among the many factors that exhibit RNA-dependency with regards to their protein interactome[41]. While these studies have underscored the potential roles of TOP1 as an RNA-binding protein (RBP), the analysis of various classes of transcripts that are in association with TOP1 and the functional consequences of these complexes remain unexplored.

In this study, we characterize TOP1 as an RBP by demonstrating its ability to form direct and physiological associations with various classes of RNAs. Our analyses reveal that TOP1

associates with RNAs that are transcribed from intergenic and promoter regions. Importantly, this phenomenon occurs with RNAs transcribed both within the nucleolus where TOP1 primarily localizes and in the nucleoplasm following acute TNF-α signaling in colon cancer cells. Additionally, we provide evidence that RNAs play a key role in maintaining the integrity of TOP1-containing ribonucleoprotein complexes and in particular those that are crucial for pre-rRNA processing in the nucleolus.

Results

TOP1 interacts with different classes of RNAs

TOP1 exerts a critical role in transcription regulation in response to various stimuli that include DNA damage induced by UV radiation and androgen-receptor signaling[23, 24, 42]. The sensitivity of TOP1 to the cellular context together with its requirement in the acute transcription response[23], prompted us to explore the ability of TOP1 to associate with RNAs in response to acute immune signaling in colon cancer cells. Consistent with this possibility, previous studies have identified TOP1 as a non-canonical mRNA-binding protein in a global survey of proteins and as a component of ribonucleoprotein complexes that consist of the *NORAD* lncRNA[37, 38, 40]. Therefore, we performed ultraviolet-crosslinked RNA immunoprecipitation (UV-RIP) using an antibody against TOP1 in SW480 cells treated with tumor necrosis alpha (TNF-α) for 1h. Consistent with the transcriptional role and localization of TOP1 in the nucleolus and nucleoplasm, TOP1 was coimmunoprecipitated with RNAs transcribed in both nuclear subcompartments (Fig. 1a). As shown in Fig. 1a, TOP1 was found in association with nucleoplasmic RNAs that include the protein coding *CSF2* mRNA and the intergenic *CSF2* eRNA and *NORAD* lncRNA. In addition, the nucleolar RNAs such as the 18S rRNA, 45S rRNA and U8 snoRNA were also coimmunoprecipitated with TOP1 (Fig. 1a).

To investigate direct RNA binding by TOP1, we performed RNA electrophoretic mobility shift assays (EMSAs) using full-length human TOP1 expressed and purified from Sf9 cells (Supplementary Fig. 1a). Specifically, the RNA EMSA was performed with increasing doses of TOP1 and equimolar amounts of an in vitro-transcribed and ^{32}P-labeled RNA. As shown in Fig. 1b, TOP1 not only directly interacts with its well-known DNA substrate, but also was found to directly interact with RNA as revealed by the formation of a distinct migrating TOP1-RNA

complex. Notably, the smearing of the bands corresponding to the TOP1-RNA complexes was consistent among the experimental replicates. As previously reported[43], this EMSA profile is indicative of multiple TOP1 molecules interacting with various regions of a single RNA molecule. Consistent with our RNA EMSA experiments and UV RIP data, we also found that TOP1 directly interacts with different RNAs as examined through *in vitro* RNA pull-down assays. As shown in Fig. 1c, recombinant TOP1 protein directly bound to *in vitro*-transcribed RNA probes of various sequences derived from the nucleolar genomic region corresponding to the 45S rDNA (RNA1) and nucleoplasmic regions that include the *CCL2* (RNA2) and *MMP9* (RNA3) enhancers. This finding that TOP1 interacts with multiple RNA species is consistent with TOP1-RNA interactions being sequence-independent. Altogether, these results identify TOP1 as an RNA-binding factor and demonstrate its ability to directly interact with different classes of RNAs.

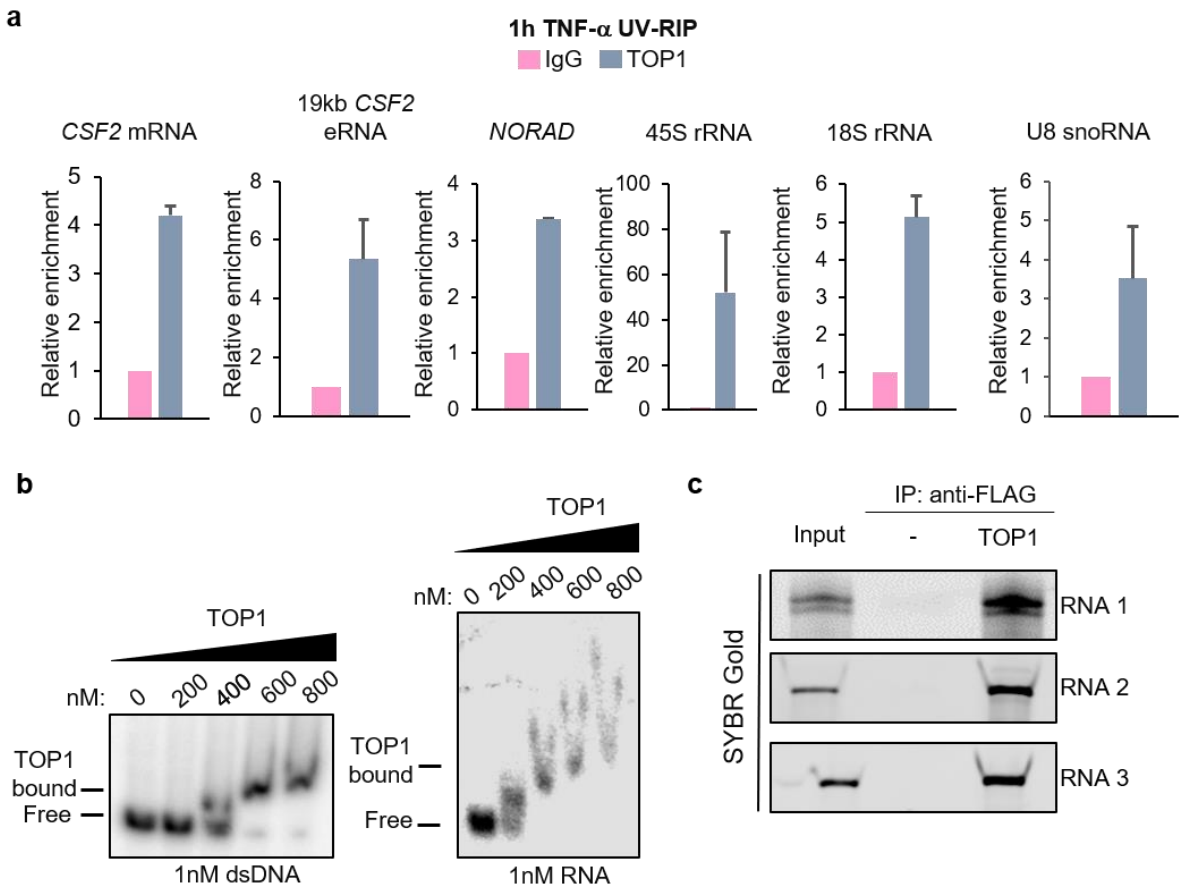

Figure 1. TOP1 interacts with different classes of RNAs
a) (Top) qRT–PCR of *CSF2* eRNA and mRNA, *NORAD* lncRNA, 18S rRNA, 45S rRNA and U8 snoRNA following UV-RIP with IgG and TOP1 antibodies in SW480 cells treated with TNF-α for 1h. Enrichment levels are relative to IgG, and data represent the mean and s.e.m of n=2 that are representative of at least three independent replicates. **b)** EMSA performed with 1nM of ^{32}P-labeled 286-nt double-stranded DNA (dsDNA) probe (left) and the corresponding in vitro-transcribed 286-nt RNA probe (right) where both TOP1-nucleic acid binding reactions were resolved on the same gel. **c)** *In vitro* pulldown of *in vitro*-transcribed RNA probes corresponding to regions of the 45S rRNA (RNA 1), *CCL2* eRNA (RNA 2) and *MMP9* eRNA (RNA 3) with FLAG-tagged TOP1 protein as revealed by SYBR Gold staining. n=3 independent experiments for **b** and **c**. n=3 for all EMSA and RNA in vitro pull-down experiments.

RNAs inhibit TOP1 catalytic activity *in vitro*

Having found that TOP1 interacts with RNAs, we hypothesized that associations with an additional nucleic acid could impact TOP1 engagement onto DNA. Our EMSA experiments together with i*n vitro* RNA pull-down assays revealed that TOP1 directly interacts with RNAs in a sequence independent manner (Fig. 1c). Therefore, as shown in Fig. 2a, TOP1 DNA-relaxation assays were performed by pre-incubating TOP1 with plasmid DNA for 5 minutes followed by the addition of increasing doses of *in vitro*-transcribed probes corresponding to RNAs 3 and 4. As a result, we found that TOP1catalytic activity is inhibited as revealed by the accumulation of the supercoiled plasmid fraction with increasing doses of RNA (Fig. 2a). Importantly, the RNA-mediated inhibition of TOP1 catalytic activity was observed with as low as a 1:1 molar ratio between RNA and DNA (Fig. 2a). To study the effect of RNAs in TOP1 catalytic activity in cells, our previously characterized *CCL2* enhancer[44] was selected as a target to assess TOP1 catalytic engagement using a variation of the established TOP1-seq methodology[22]. Briefly, human SW480 colon cancer cells were untreated or treated with TNF-α for 1h followed by a short 4-minute treatment with the TOP1-selective inhibitor, CPT (Fig. 2b). This brief CPT treatment traps the enzyme in its TOP1cc intermediate without altering TOP1 protein levels (Supplementary Fig. 2a) or the chromatin state[22]. In turn, this method followed by qPCR allows for the immunoprecipitation of only catalytically engaged TOP1 (TOP1cc). While TOP1 protein levels remained unchanged (Supplementary Fig. 2b), a significant increase in TOP1 catalytic engagement was observed in response to acute TNF-α signaling at the *CCL2* enhancer (Fig. 2c).

If the RNA indeed acts as an inhibitory factor for TOP1 catalytic activity in the cell as revealed by our *in vitro* studies, we hypothesized that reducing the *CCL2* eRNA levels would cause an increase in TOP1 catalytic engagement at the *CCL2* enhancer. To test this, antisense

oligonucleotides (ASOs) were used to target the *CCL2* eRNA in SW480 cells following 1h TNF-α treatment which is the condition in which we found TOP1 to be highly enzymatically active. Relative to a non-targeting ASO (Ctrl), the *CCL2* ASO reduced the *CCL2* eRNA levels by 66% followed by a reduction in the *CCL2* mRNA levels by 40% while the *MMP9* eRNA remained unaffected (Fig. 2d). Next, immunoprecipitation of TOP1cc followed by qPCR was performed in SW480 cells treated with 1h TNF-α following the ASO-mediated knockdown of the *CCL2* eRNA. Unexpectedly, TOP1 engagement at the *CCL2* enhancer remained unaffected despite a significant decrease in the *CCL2* eRNA levels (Fig. 2e). This data suggests that TOP1-RNA interactions may not directly impact TOP1 engagement on the DNA at the *CCL2* enhancer. However, a global assessment of the RNA-mediated inhibition of TOP1 catalytic activity is required to find genomic loci at which this mechanism is impacting TOP1 engagement.

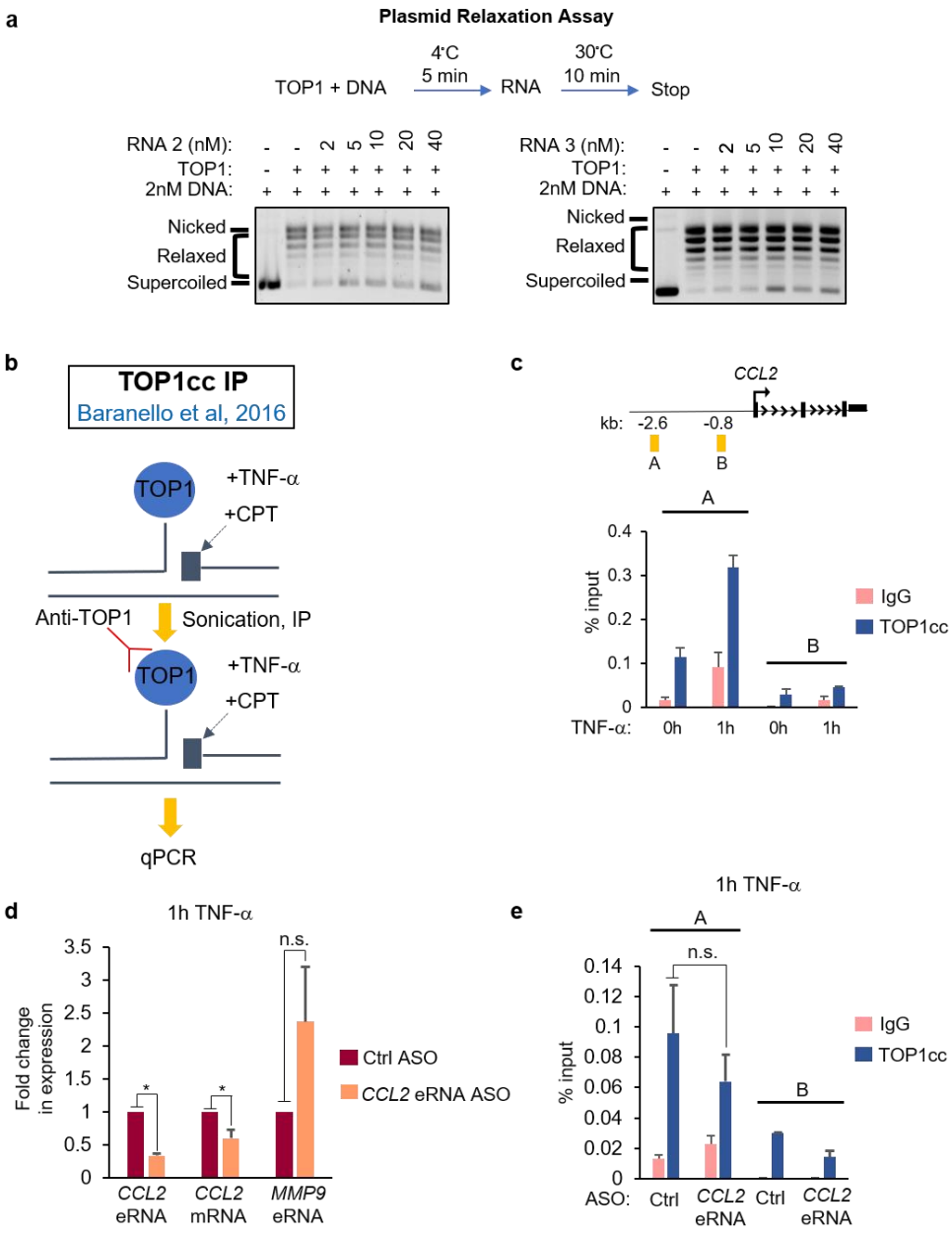

Figure 2. RNAs inhibit TOP1 catalytic activity *in vitro*.
a) Plasmid relaxation assay with TOP1 pre-incubated with 2nM plasmid DNA for 5min followed by the addition of increasing amounts of *in vitro*-synthesized RNA probes corresponding to regions of the *CCL2* eRNA (RNA 2) and *MMP9* eRNA (RNA 3). Samples were subjected to 0.8% agarose gel electrophoresis and visualized by staining with ethidium bromide. **b)** Schematic of the TOP1cc immunoprecipitation methodology adapted from TOP1-seq[22] **c)** Schematics of qPCR amplicons (top) and analyses (bottom) of IgG and TOP1cc at the enhancer (amplicon A) and nonspecific (amplicon B) regions of the *CCL2* gene locus in SW480 cells untreated (0h) or treated with TNF-α for 1h. **d)** qRT–PCR of SW480 cells treated with a control (ctrl) or *CCL2* eRNA ASO and TNF-α for 1h. Expression levels are relative to the control experiments and data represent the mean and s.e.m. of $n = 3$ independent experiments. **e)** TOP1cc IP analyses of IgG and TOP1cc at the *CCL2* regions denoted in **c** in SW480 cells treated with ctrl or *CCL2* eRNA ASO and TNF-α for 1h. In **c** and **e**, data represent the mean and s.e.m. of $n = 3$ independent TOP1cc IP experiments. Statistical significance was determined by two-tailed Student's *t* test. $^*P < 0.05$. n=3 for the plasmid relaxation assay and RNA in vitro pull-down experiments.

TOP1 forms RNA-dependent protein complexes

To gain insights into the mechanisms underlying RNA functions through interactions with TOP1, we next investigated the role that RNA plays in regulating the protein interactome of TOP1. Recently, an unbiased proteome-wide screen identified TOP1 to be among a group of proteins whose interactome is dependent on RNA as defined by TOP1's differential migration pattern in a sucrose density gradient in the presence versus absence of RNAs[41]. While this study reported a group of proteins co-migrating with TOP1 in an RNA-dependent manner, we sought to further identify the proteins that are specifically interacting with TOP1 in response to acute TNF-α signaling where we found TOP1 in association with various RNAs. Therefore, we similarly fractionated TOP1 by sucrose density gradient ultracentrifugation from untreated and RNase-treated whole cell lysates obtained from SW480 cells following 1h TNF-α treatment. Treatment with a pool of RNase enzymes resulted in the efficient degradation of RNAs (Supplementary Fig. 3a). As shown in Fig. 3a and consistent with the previous report[41], immunoblot analysis of the collected sucrose fractions revealed an RNA-dependent shift in which TOP1 distribution in the higher versus lower sucrose density fractions are well separated. Specifically, we found that TOP1 distribution in the untreated samples was found primarily in the higher sucrose density fractions 15 to 23. In comparison, RNase treatment resulted in TOP1 redistribution towards the lower sucrose density fractions 5 to 10 (Fig. 3a).

To identify the specific proteins that interact with TOP1 in an RNA-dependent manner, we coupled our sucrose density gradient ultracentrifugation with TOP1 immunoprecipitation followed by mass spectrometry (IP-MS). As depicted in Fig. 3b, the untreated (19-23) and RNase-treated (6-10) fractions where high levels of TOP1 were detected by immunoblot analysis following the sucrose density gradient ultracentrifugation in 1h TNFα-induced conditions were pooled together.

The pooled fractions were subsequently used for immunoprecipitation with TOP1 or nonspecific IgG antibodies and the isolated proteins were analyzed by gel electrophoresis followed by silver staining or liquid chromatography and mass spectrometry (LC/MS) analyses (Fig. 3b). The silver stain analysis demonstrated a specific enrichment of TOP1-associating proteins as compared to the IgG control (Fig. 3c). Furthermore, the significant decrease or loss of several factors was observed in the TOP1 IP with RNase-treated conditions as compared to the untreated conditions (Fig. 3c).

Two independent replicates were processed for LC/MS analysis where only resulting factors shared among both replicates with a $-\log_{10}$ p-value above 30 and those found to be 2-fold higher in the TOP1 as compared to the IgG immunoprecipitation were further processed for analyses. A total of 14 proteins in association with TOP1 were identified in the untreated conditions while 10 proteins were immunoprecipitated with TOP1 following the RNase treatment (Fig. 3d). Two factors that include TOP1 and mitochondrial TOP1 were present in the untreated and RNase-treated conditions. As a result, 12 proteins were uniquely identified in association with TOP1 in the untreated conditions and not found following the RNase treatment (Table 1, Fig. 3d). Moreover, 8 proteins (TCOF, IWS1, RPGF3, KAPCB, KAPCA, KI67, RLA0 and RLA0L) were uniquely immunoprecipitated with TOP1 following the RNase treatment (Table 2, Fig. 3d). The TCOF protein is previously reported as a component of the Nop56p-associated pre-rRNA complex together with TOP1, suggesting that both factors play a role in pre-rRNA processing[45]. Similarly to TOP1, IWS1 is found in association with RNAPII and is also an important regulator of the RNAPII-elongation complex[22, 46].

As shown in Fig. 3e, TOP1 protein interactome networks were generated using the STRING database with the 12 RNA-dependent TOP1-associating proteins. This analysis identified

6 out of the 12 proteins (NPM1, MYBBP1A, RPS6, RPL17, RPL29 and PLEC) as part of the TOP1 interactome network based on curated data bases, while 6 proteins (LRRK2, SLC25A3, RIF1, HSPA2, RRBP1, ZNF638) were unidentified (Fig. 3e). Similarly to TOP1, NPM1 and MYBBP1A have been directly linked to mechanisms in the nucleolus surrounding rDNA transcription. NPM1 stimulates rRNA synthesis by binding to rDNA promoters and by exerting its histone chaperone activity[47] while MYBBP1A is a repressor of rDNA transcription[48]. TOP1-NPM1 associations are further reported in global proteomic analysis[49, 50]. While HSPA2 was among the unidentified proteins, early studies revealed that HSPA2 is a regulator of apoptosis that interacts with TOP1 whose activity was further found to contribute to the transcription of the HSPA2 gene in Drosophila[51, 52]. In addition, RIF1 is a non-homologous end-joining (NHEJ) factor that assists in the repair of DSBs resulting from stalled replication forks[53]. TOP1-RIF1 associations have not been reported, however TOP1 is key in modulating DNA supercoiling during DNA replication that could otherwise lead to DSBs that could subsequently be repaired by RIF1[4].

Gene Ontology (GO) analysis of the RNA-dependent TOP1-interacting proteins revealed that 5 are involved in the Nop56p-associated pre-rRNA complex (NPM1, RPL17, RPL29, RPS6 and MYBBP1A), 3 in ribosome biogenesis (NPM1, RPS6 and MYBBP1A), 3 in positive regulation of cell cycle process (HSPA2, NPM1 and MYBBP1A) and 3 in the regulation of cellular response to stress (NPM1, RIF1 and LRRK2) (Fig. 3f). TOP1 was previously identified as a component of the Nop56p-associated pre-rRNA complex together with NPM1 and MYBBP1A[45] where they were classified as transcriptional regulators and non-ribosomal proteins. The identification of the Nop56p-associated pre-rRNA complex as the highest enriched pathway through GO analysis is in accordance with our STRING analysis where the proteins associated with this complex were identified as the known functional binding partners of TOP1 (Fig. 3e). To

further validate the TOP1-associating proteins identified via LC/MS, we immunoprecipitated TOP1 from 1h TNF-α-treated SW480 whole cell lysates that were untreated or RNase-treated. In accordance with our LC/MS results, we found that TOP1-NPM1 associations were significantly decreased following the degradation of RNAs (Supplementary Fig. 4). Our proteomic analyses have uncovered a role for RNAs in regulating the ability of TOP1 to assemble ribonucleoprotein complexes which contribute to the well-known mechanisms that are regulated by TOP1.

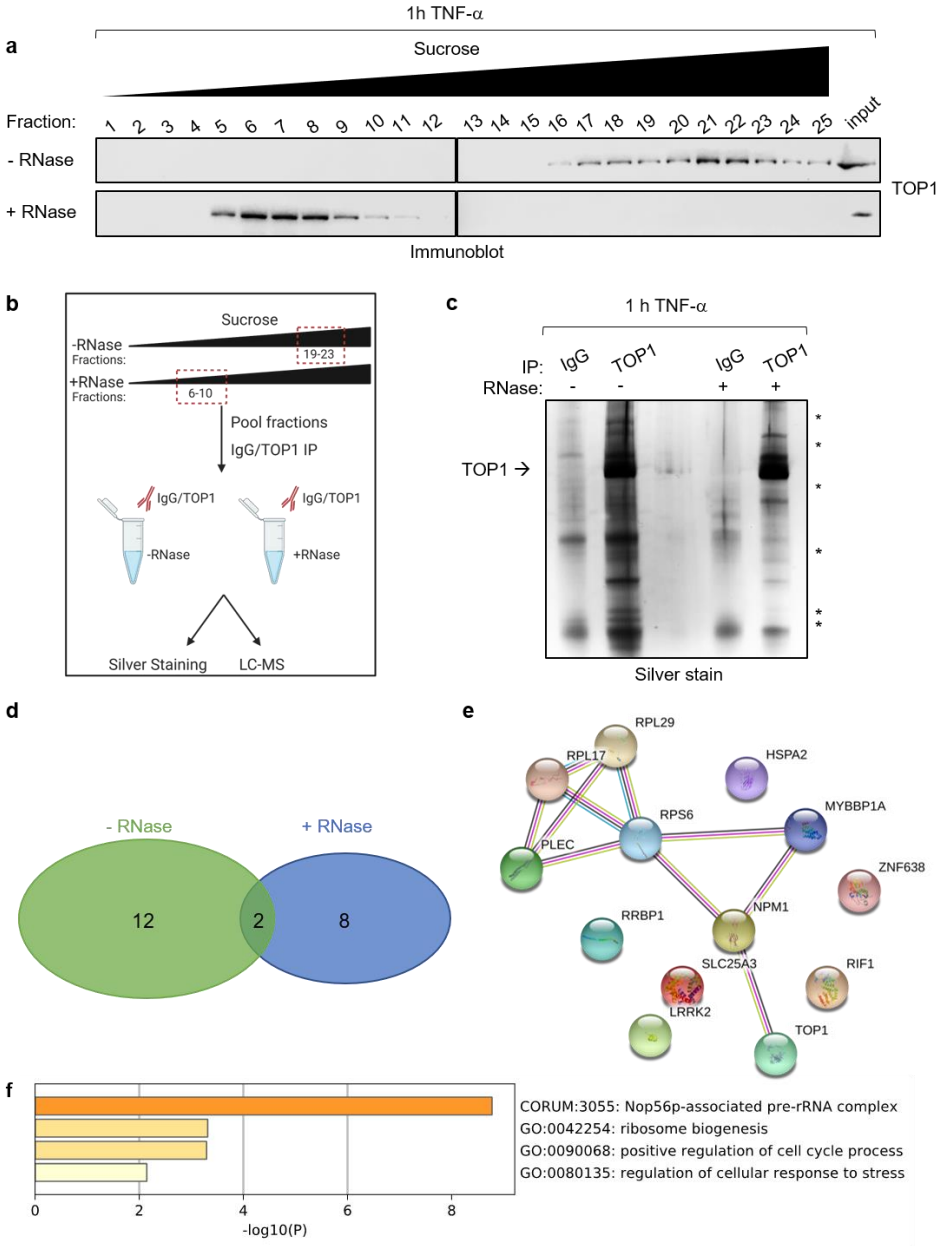

Figure 3. TOP1 forms RNA-dependent protein complexes.
a) TOP1 immunoblot analysis of the protein amount present in the 25 collected fractions following sucrose density centrifugation from untreated or RNase-treated whole cell lysates from SW480 cells treated with 1h TNF-α. n=3 independent experiments. **b)** Schematic overview of TOP1 IP from sucrose fractions followed by mass spectrometry in untreated or RNase-treated conditions. **c)** Silver stain analysis following immunoprecipitation using IgG or TOP1 antibodies from the untreated or RNase-treated sucrose fractions containing TOP1 as shown in a and b. Asterisks (*) denote significantly decreased or loss bands in TOP1 IP in response to RNase treatment. n=3 independent repeats. **d)** Venn diagram indicating the number of TOP1-associating proteins uniquely enriched for the untreated, RNase-treated or both samples following LC/MS analysis. **e)** Protein network analysis using STRING and **f)** Gene Ontology (GO) analysis using Metascape of the 13 proteins whose association with TOP1 was lost in the RNase-treated sample compared to the untreated sample as revealed by LC/MS analysis. Proteins in the STRING analysis are presented by network nodes of different colors. The edges between TOP1 and its predicted binding partners represent protein-protein associations. Identified interactions are found from experimental results or curated databases. In **d-f**, data represent 2 independent experiments.

Discussion

TOP1 resolves topological constraints resulting from separation of DNA strands during replication and transcription. Given the ability of this enzyme to introduce transient yet detrimental DNA nicks, understanding the previously unrecognized mechanisms that regulate TOP1 function is of great significance. This study advances our current understanding of the regulatory roles of TOP1 by characterizing this factor as a noncanonical RBP. Notably, we have identified the ability of TOP1 to form associations with different classes of RNAs that include protein-coding mRNAs as well as a wide array of noncoding transcripts. Moreover, our data underscores the importance of RNA interactions for maintaining TOP1's protein interactome.

Having established that RNA interactions add an additional layer of complexity to TOP1 regulation, further identification of RNA binding regions (RBRs) within this protein is essential to explore the clinical implications of TOP1 targeting in cancer treatment. Recent unbiased and high resolution mapping of RBRs in nuclear proteins using mouse embryonic stem cells not only classified TOP1 as an RBP, but further identified a 13-amino acid peptide that lies within its DNA-binding domain (DBD) as the RBR[39]. While further validation and in vitro characterization of this 13-residue RBR is needed, it is highly plausible that the same peptide region in human TOP1 would also support RNA binding given its complete sequence conservation from mice to humans. Notably, RNAs interacting with TOP1 through its DBD could be significant with regards to TOP1 targeting given that the current chemotherapeutic agents against TOP1 stabilize its covalent engagement on DNA.

Our *in vitro* analyses of TOP1 enzymatic activity have provided insights into the ability of RNA to inhibit TOP1 catalytic activity. Our efforts to further dissect this mechanism in colon cancer cells using ASOs to specifically target the *CCL2* eRNA did not reveal changes in TOP1

catalytic engagement at the *CCL2* enhancer. However additional genome-wide approaches are necessary to globally assess TOP1 engagement and to manipulate the levels of various transcripts. Recent studies reported that the RNA exosome reduces the levels of non-coding RNAs and its mutagenesis or knockdown results in increased levels of these transcripts[36, 54, 55]. In this study we have reported that TOP1 associates with various non-coding transcripts. Therefore, manipulation of the RNA exosome followed by an assessment of TOP1 catalytic engagement could provide genome-wide insights into the potential effect of RNAs in TOP1 enzymatic activity.

TOP1 activity exerts a crucial role in modulating the DNA supercoiling state to promote transcription initiation and RNAPII elongation[8, 22]. Interestingly, transcriptional bursting has been defined as an additional regulatory layer of gene expression in which RNA production occurs in a discontinuous fashion during short yet strong periods followed by periods of inactivity[56-58]. Single-cell analyses reveal that cellular stimuli that lead to an acute transcriptional response increase the transcription rate and burst size resulting in an increase in gene expression[59]. We have found that TOP1 associates with RNAs in response to stimulus driven by acute TNF-α signaling. Therefore, the inhibition of TOP1 activity by RNAs could be a relevant mechanism at highly transcribed genomic loci in response to acute TNF-α signaling. RNAs may act as an inhibitory factor of TOP1 activity that contributes to the reported decrease in its catalytic activity that is observed at transcriptional start sites[22]. Consequently, TOP1-RNA interactions could directly modulate the DNA topological state to drive transcription initiation during the various transcriptional burst periods and contribute to an increase in gene expression.

In accordance with previous studies[41], our proteomic data establishes the essential role of RNAs in maintaining several TOP1-protein associations. Consistent with the predominant

localization of TOP1 in the nucleolus[11], our GO analysis revealed that a significant amount of the RNA-dependent TOP1-associating proteins are involved in biological pathways known to occur within the nucleolus. These pathways include the Nop56-associated pre-rRNA complex and ribosome biogenesis. Among these proteins, we found components of the 40S (RPS6) and 60S (RPL17 and RPL29) ribosomal subunits which are conventionally known to be found in the cytoplasm. A study reported for the first time that rRNA and protein components of the ribosome are globally found at transcriptionally active sites[60]. Given the direct role of TOP1 in the nucleus as an important transcriptional cofactor, TOP1-RNA associations at transcribed regions could be promoting the localization of ribosomal subunits at these loci. Importantly, factors whose association with TOP1 is RNA-dependent, namely the protein components of the ribosome and NPM1, are also known to associate with RNAs[61-63]. Therefore, further studies are required to determine whether the observed RNA-dependent associations are mediated directly by the RNA-binding property of TOP1.

Interestingly, the TOP1 RNA-dependent protein complexes that we identified may be contributing to the membraneless structure of the nucleolus. The nucleolus exhibits a liquid-like phase separated conformation where RNAs and intrinsically disordered region (IDR)-containing proteins form a complex network that supports ribosome biogenesis and pre-rRNA processing reactions[64, 65]. TOP1 possesses unexplored properties that could attribute the enzyme with a function in phase separation. Namely, studies have characterized the N-terminal domain (NTD) of TOP1 as an intrinsically disordered region (IDR) that contains specific nuclear and nucleolar localization signals important for the enzyme's localization[66-69]. Additionally, TOP1 has been directly shown to play a role in the maintenance of the nucleolar morphology[19] and our study now establishes the ability of TOP1 to interact with nucleolar RNAs. TOP1-RNA associations together

with the TOP1 RNA-dependent protein complexes may contribute to the phase-separated nature of the nucleolus to and support the high protein synthesis demand of rapidly dividing cancer cells.

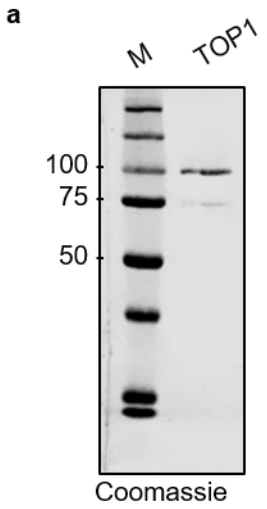

Supplementary Figure 1. Recombinant human FLAG-TOP1
a) Recombinant human FLAG-TOP1 analyzed by Coomassie staining

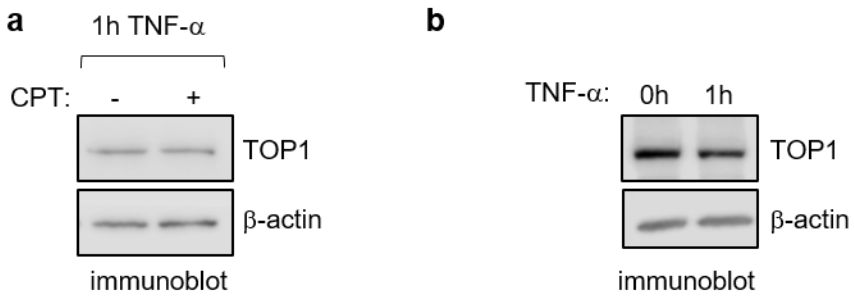

Supplementary Figure 2. TOP1 immunoblots following CPT and TNF-α treatments
a)Immunoblot analysis of SW480 cells treated with TNF-α for 1h and treated or untreated with CPT for 4min. (n=3 experiments) **b)** Immunoblot analysis of SW480 cells treated with TNF-α for 0h or 1h. (n=3 experiments)

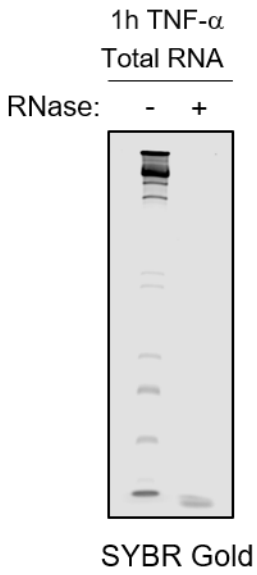

Supplementary Figure 3. Total RNA following RNase treatment
a) Total RNA extracted from SW480 cells treated with TNF-α for 1h and untreated or treated with RNase A, RNase I, RNase T1 and RNase H.

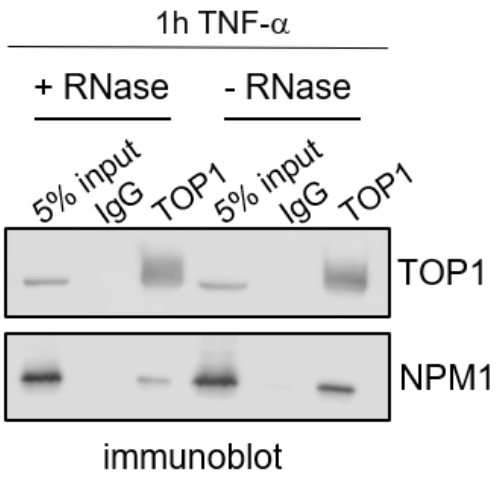

Supplementary Figure 4. TOP1-NPM1 RNA-dependent associations
a) Co-immunoprecipitation of TOP1 and NPM1 from whole cell lysates extracted from SW480 cells treated with TNF-α for 1h and untreated or treated with RNase A, RNase I, RNase T1 and RNase H.

Table 1. TOP1-associating proteins determined by TOP1 IP followed by LC/MS in untreated conditions

Protein ID	MW (kDa)	$-\log_{10}$ p value
Q9P2E9|RRBP1_HUMAN	152.472	115.78
Q14966|ZN638_HUMAN	220.623	98.13
Q00325|MPCP_HUMAN	40.095	48.60
P54652|HSP72_HUMAN	70.021	63.36
P47914|RL29_HUMAN	17.752	51.61
P06748|NPM_HUMAN	32.575	73.18
Q9BQG0|MBB1A_HUMAN	148.854	41.18
Q5UIP0|RIF1_HUMAN	274.464	42.19
P62753|RS6_HUMAN	28.681	36.92
Q15149|PLEC_HUMAN	531.796	32.99
P18621|RL17_HUMAN	21.397	38.99
Q5S007|LRRK2_HUMAN	286.100	87.44

Table 2. TOP1-associating proteins determined by TOP1 IP followed by LC/MS in RNase-treated conditions

Protein ID	MW (kDa)	$-\log_{10}$ p value
Q13428|TCOF_HUMAN	152.105	174.7
Q96ST2|IWS1_HUMAN	91.955	118.8
O95398|RPGF3_HUMAN	103.751	108.9
P22694|KAPCB_HUMAN	40.623	79.39
P17612|KAPCA_HUMAN	40.590	81.91
P46013|KI67_HUMAN	358.695	81.40
P05388|RLA0_HUMAN	34.274	99.94
Q8NHW5|RLA0L_HUMAN	34.364	98.48

Materials and Methods

Antibodies. The antibodies used for IP analyses were obtained as follows: anti-TOP1 (ab219735, 2 μg) from Abcam and anti-IgG (2729, 2 μg) from Cell Signaling Technology. The antibodies used for immunoblotting analyses were obtained as follows: anti-TOP1 (sc-32736 1:1000 dilution) and anti-β-actin (sc-47778 1:2000 dilution) from Santa Cruz Biotechnology.

RNA Purification and qRT-PCR. Total RNA was extracted from SW480 cells using TRIzol reagent (Invitrogen) and 1 μg of total RNA was used for cDNA synthesis using the ProtoScript II First Strand cDNA Synthesis Kit (NEB). PCR reactions were set up using SYBR Green PCR Master Mix (Applied Biosystems) on an Applied Biosystems Step One Plus real-time PCR systems. The specificity of amplification was confirmed by melting curve analysis and the RNA expression levels were calculated using the ddCt method normalized to *GAPDH*. The expression levels in ASO knockdown condition are relative to the control knockdown levels. For UV-RIP analyses, RNA enrichment in IgG and TOP1 IP samples was normalized to *GAPDH* from input samples. Primers for qRT-PCR are listed in Supplementary Table 2.

Immunoblotting. SW480 cells were lysed in lysis buffer (20 mM Tris HCl pH 7.5, 300 mM NaCl, 2 mM EDTA, 0.5% NP40, 1% Triton-X) for 30 min on ice. The protein concentration from cleared cell lysates was determined using Bio Rad Protein Assay Dye Reagent (Bio-Rad Laboratories). Protein samples denatured at 95 °C for 5 min were separated by SDS-PAGE and transferred to PVDF membranes (EMD Millipore). The membranes were blocked in 3% milk and probed with the indicated antibodies. Reactive bands were detected by ECL reagent and visualized using LI-COR Odyssey Fc Imaging System.

Ultraviolet-RNA Immunoprecipitation (UV-RIP). 20 million SW480 cells that were untreated or treated with 12.5 ng mL^{-1} TNF-α for 1h were crosslinked by UV irradiation (150 mJ per cm^2 at 254 nm) using a Stratalinker. The cells were lysed in RIP lysis buffer [25 mM HEPES-KOH pH 7.5, 150 mM KCl, 0.5% NP40, 1.5 mM $MgCl_2$, 10% glycerol, 1 mM EDTA, 0.4 U RNaseOUT (Thermo Fisher Scientific), protease inhibitor cocktails (PICs)] on ice for 30 min and cleared cell lysates were used for IP with TOP1 and IgG-antibody bound Protein A Dynabeads (Invitrogen) for 12-16 h. Beads were subsequently washed three times with RIP lysis buffer and RNA samples were eluted using TRIzol LS reagent (Invitrogen). cDNA samples were prepared as described above and analyzed by qRT-PCR primers listed in Supplementary Table 2.

***In vitro* RNA synthesis**. Primers were designed to amplify desired genomic regions that correspond to *NORAD, 45S* rDNA, *CCL2* eRNA and *MMP9* eRNA. The T7 promoter sequence was added to the forward primer for amplification from cDNA synthesized from SW480 colon cancer cells. The primers used for PCR amplification can be found in Supplementary Table 1. The amplified DNA was subsequently used for RNA synthesis using the T7 RiboMAX Express Large-Scale RNA Production System (Promega) followed by purification with MicroSpin G-25 Columns (GE Healthcare Life Sciences). RNAs were quantitated by Nanodrop (Invitrogen) and their integrity was verified on a 5% TBE urea gel followed by staining with SYBR Gold (Life Technologies) for 20 min prior to imaging using LI-COR Odyssey Fc Imaging System.

RNA probes were refolded by incubation at 85°C for 2 min followed by a 10-fold dilution with cold RNA refolding buffer (10 mM Tris-HCl pH 7, 10 mM $MgCl_2$, 100 mM KCl) and snap-cooling on an ice-cold metal rack for 5 min. RNAs were allowed to refold by bringing the sample to room temperature for 30 min.

Electrophoretic Mobility Shift Assays. EMSAs were performed based on established protocols with a few modifications[70]. The 286 bp DNA probes were generated by PCR using primers amplifying the *CCL2* enhancer region corresponding to the maximal RNA peak according to our published GRO-seq data[44]. The 286 bp DNA product was used as the template for T7-synthesis of the RNA probe. Labeling reactions were carried out with 10 pmol of DNA or 10 μg of RNA, T4 polynucleotide kinase (NEB) and γ-^{32}P-ATP (Perkin Elmer). Unincorporated γ-^{32}P-ATP was removed from DNA by purification with MicroSpin G-25 Columns (GE Healthcare Life Sciences) and from RNA by extraction from 5% TBE urea gel using the ZR small-RNA PAGE Recovery Kit (Zymo Research). Labeled samples were quantified by running known amounts of unlabeled nucleic acid on an agarose gel for DNA or 5% TBE urea gel for RNA. Standard curves were generated following the quantification of the intensity of the nucleic acid bands using ImageJ.

Binding reactions were performed using 1 nM of labeled nucleic acids in 1X EMSA buffer [20 mM Tris-HCl pH 7.4, 100 mM KCl, 1mM EDTA, 1% glycerol, 0.05% NP40, 0.5 mM ZnCl2, 0.1 mg mL^{-1} BSA (Fisher), 0.1 mg mL^{-1} yeast tRNA (Sigma), 2 mM DTT) supplemented with 0.4U RNaseOUT (Thermo Fisher Scientific)] for RNA EMSAs. The RNA probe was refolded prior to addition to the reaction. The binding reactions were initiated by the addition of various doses (200-800 nM) of FLAG-TOP1 protein and incubation at 4°C for 30 min. Reactions were loaded on a 4% native polyacrylamide gel that was pre-chilled overnight and pre-run for 1 h at 150V. The gel was run for 4 h at 150V and exposed to autoradiography screen for 12-16 h prior to imaging with Typhoon phophorimager.

In vitro pull-down RNA binding assays. Binding reactions were set up using 200 ng of FLAG-tagged proteins and 1 μg of refolded RNA in RNA binding buffer (20 mM Tris-HCl at pH 7.4, 100 mM KCl, 0.2 mM EDTA, 0.05% NP40, 0.4 U RNase inhibitor, PICs) and incubated at

4°C for 1h. Protein-RNA complexes were recovered using FLAG M2 agarose beads for 1h at 4°C. Beads were washed three times with RNA wash buffer (20 mM Tris-HCl at pH 7.4, 200 mM KCl, 0.2 mM EDTA, 0.05% NP40, PICs) and RNA samples were eluted using TRIzol LS reagent. Purified RNA samples were resolved on a denaturing 5% TBE urea gel and stained with SYBR gold for 20 min before imaging using LI-COR Odyssey Fc Imaging System.

DNA Supercoiling Assay. DNA supercoiling assays were performed based on established protocols[71]. Briefly, 2 nM of TOP1 was incubated with various amounts of refolded RNA (2-40 nM) on ice for 5 min in 1X TOP1 buffer (25 mM HEPES pH 7.6, 100 mM KCl, 0.2 mM $MgCl_2$, 0.1 mM EDTA and 10% glycerol) in a final volume of 50 μL. Following the addition of 2 nM plasmid DNA, reactions were incubated at 30°C for 10min. The reactions were deproteinized by the addition of 12.5 μg of Proteinase K (Life Technologies) at 45°C for 10 min. Purified DNA was subjected to 0.8% agarose gel electrophoresis at 120 V for 90 min and stained with EtBr for 20 min prior to imaging using LI-COR Odyssey Fc Imaging System

TOP1cc IP. TOP1cc IP was adapted from the TOP1-seq established protocol[22]. 20 – 24 million SW480 cells that were untreated or treated with 12.5 ng mL^{-1} TNF-α for 1h, followed by a 4-min treatment with 10 μM CPT. Cells were immediately washed with ice-cold 1X PBS, scraped, resuspended in lysis buffer (20 mM Tris-HCl pH 7.5, 300 mM NaCl, 2 mM EDTA, 0.5% NP40, 1% Triton X-100, 1 mM PMSF, PICs), and incubated on ice for 15 min. Cell resuspensions were dounced ten times using an ice-cold glass homogenizer. Nuclei were collected by centrifugation and resuspended in shearing buffer (0.1% SDS, 0.5% N-lauroylsarcosine, 1% Triton X-100, 10 mM Tris-HCl pH 8.1, 100 mM NaCl, 1 mM EDTA, 1 mM PMSF, PICs). Chromatin was fragmented using a bioruptor Pico sonicator (Diagenode) to an average size of 200-600 bp and cleared chromatin was used for immunoprecipitation overnight at 4 ºC with protein A

Dynabeads that were pre-coupled in 0.5% BSA with IgG or TOP1 antibodies. The immunocomplex-bound beads were washed eight times in wash buffer (50 mM HEPES-KOH pH 7.6, 500 mM LiCl, 1 mM EDTA, 1% NP40, 0.7% sodium deoxycholate, 1 mM PMSF, PICs), twice in 1X TE, and eluted in elution buffer (50 mM Tris-HCl pH 8.0, 10 mM EDTA, 1% SDS). Immunoprecipitated DNA samples were purified using DNA Clean & Concentrator Kit (Zymo Research) and analyzed by RT-PCR using primers in Supplementary Table 2.

ASO transfection. 100 nM non-targeting (control) or *CCL2* eRNA ASOs (Integrated DNA Technologies) (Supplementary Table 3) were heated at 75 °C for 6 min and SW480 cells were transfected using Lipofectamine 3000 (Life Technologies). Cells were treated with 12.5 ng mL^{-1} TNF-α for the indicated time points 16h post-transfection and harvested for RNA expression analyses and TOP1cc IP.

SW480 cell lysate preparation for sucrose density gradient ultracentrifugation. This assay was performed following previously established protocols[41]. 20 – 24 million SW480 cells that were untreated or treated with 12.5 ng mL^{-1} TNF-α for 1h were harvested and collected by centrifugation. Cell pellets were resuspended in 150 µL of lysis buffer (20 mM Tris-HCl pH 7.5, 300 mM NaCl, 2 mM EDTA, 0.5% NP40, 1% Triton X-100, 1 mM PMSF, PICs), incubated on ice for 30 min, and gently vortexed every 5 min. Cell resuspensions were next snap frozen in liquid nitrogen and quickly thawed twice to fully lyse the cells. Lysates were cleared by centrifugation at 13,000 rpm for 10 min at 4 ºC and protein concentrations were determined against bovine serum albumin (BSA) standard solutions.

RNase treatment of SW480 cell lysates. 2 to 2.5 mg of protein lysate that was prepared as described above was pre-incubated with 50 µg RNase A (Fisher Scientific), 50 U RNase I (Life

technologies), 5000 U RNase T1 (Sigma), and 50 U RNase H (NEB) at 4°C for 1 h. 50 µL of lysis buffer was added to control samples and incubated at 4°C for 1h.

Sucrose density gradient ultracentrifugation. To prepare the sucrose density gradient, ten 1 mL sucrose solutions from 50% to 5% in 10 mM Tris-HCl pH 7.5, 100 mM NaCl, and 1 mM EDTA were layered on top of each other in ultra-clear tubes (Beckman Coulter) with the 50% sucrose solution on the bottom. Each layer was frozen at -80 ºC for 10 min before the addition of the next layer. Prepared sucrose gradients were stored at -20 ºC and slowly thawed at 4 ºC an hour prior to starting the spin. 2-2.5 mg of untreated and RNase-treated cell lysates were gently layered on top of the sucrose gradient without perturbing the layers. Centrifugation was performed using a Beckman ultracentrifuge with a SW41 swinging bucket rotor at 30,000 rpm for 18h at 4 ºC. Following ultracentrifugation, gradient tubes were removed from the rotor without disturbing the layers and starting from the top, 25 fractions of 400 µL each were collected into fresh 1.5 mL tubes. 5% of each fraction was taken for western blot analysis and the reminder of fractions were kept on ice until processed for immunoprecipitation.

TOP1 immunoprecipitation followed by mass spectrometry. Following immunoblot analysis of TOP1 in control and RNase-treated sucrose gradient fractions, those fractions that showed highest levels of TOP1 protein in each condition were pooled together. Pooled control (no RNase treatment) fractions were diluted twofold with 10 mM Tris-HCl pH 7.5, 100 mM NaCl, and 1 mM EDTA to adjust the sucrose concentration to the same level of the RNase-treated fractions. Protein A Dynabeads that were pre-coupled to TOP1 and IgG antibodies in 1 mg mL^{-1} BSA and crosslinked with dimethyl pimelimidate (DMP; Life technologies) were subsequently used for immunoprecipitation from the pooled sucrose fractions overnight at 4 ºC. Immunocomplexes were washed five times in ice-cold wash buffer (50 mM Tris-HCl pH 7.4, 500

mM NaCl, 0.5% sodium deoxycholate, 1% SDS, 1% NP-40) and three times in 1X PBS. After the removal of last PBS wash, protein-bound beads were either denatured at 70 ºC for 10 min for SDS-PAGE and silver stain analysis or frozen at -80 ºC for storage prior to mass-spectrometry analysis.

Sample preparation for mass spectrometry Following previously established methods[72, 73], protein samples from two biological replicates were diluted in TNE buffer (50 mM Tris-HCl pH 8.0, 100 mM NaCl, 1 mM EDTA). RapiGest SF reagent (Waters Corp.) was added to the mix to 0.1% final concentration and samples were boiled for 5 min. TCEP (Tris (2-carboxyethyl) phosphine) was added to final concentration of 1 mM and the samples were incubated at 37□C for 30 min. This was followed by carboxymethylation of samples with 0.5 mg/ml of iodoacetamide for 30 min at 37 °C and subsequent neutralization with 2 mM TCEP (final concentration). Samples were next digested with trypsin at the trypsin to protein ratio of 1 to 50 overnight at 37 °C. RapiGest reagent was degraded and removed from the samples by treating them with 250 mM HCl at 37□C for 1 h, followed by centrifugation at 14000 rpm for 30 min at 4 °C. Soluble fractions were subsequently transferred to fresh tubes and peptides were extracted using C18 desalting columns (Thermo Scientific, PI-87782). Following quantification of peptides using BCA assay, 1 μg of total peptides from each sample was injected for LC-MS analysis.

Liquid chromatography coupled with tandem mass spectroscopy (LC-MS/MS) This analysis was performed following previously established protocols[54,55]. Trypsin-digested peptides were analyzed by ultra high pressure liquid chromatography (UPLC) coupled with tandem mass spectroscopy (LC-MS/MS) using nano-spray ionization. The nanospray ionization experiments were performed using a Orbitrap fusion Lumos hybrid mass spectrometer (Thermo) interfaced with nano-scale reversed-phase UPLC (Thermo Dionex UltiMate™ 3000 RSLC nano System) using a 25 cm, 75-micron ID glass capillary packed with 1.7-μm C18 (130) BEH™ beads (Waters

corporation). Peptides were eluted from the C18 column into the mass spectrometer using a linear gradient (5–80%) of ACN (Acetonitrile) at a flow rate of 375 µl/min for 1h. The buffers used to create the ACN gradient were: Buffer A (98% H_2O, 2% ACN, 0.1% formic acid) and Buffer B (100% ACN, 0.1% formic acid). Mass spectrometer parameters were set as follows; an MS1 survey scan using the orbitrap detector (mass range (m/z): 400-1500 (using quadrupole isolation), 120000 resolution setting, spray voltage of 2200 V, Ion transfer tube temperature of 275 C, AGC target of 400000, and maximum injection time of 50 ms was followed by data dependent scans (top speed for most intense ions) with charge state set to only include +2-5 ions, and 5 second exclusion time, while selecting ions with minimal intensities of 50000 at in which the collision event was carried out in the high energy collision cell (HCD Collision Energy of 30%). The fragment masses where analyzed in the ion trap mass analyzer (With ion trap scan rate of turbo, first mass m/z was 100, AGC Target 5000 and maximum injection time of 35ms). Protein identification and label free quantification was carried out using Peaks Studio 8.5 (Bioinformatics solutions Inc.). Proteins with $-\log_{10}$ p-value of 30 and higher were retained as statistically significant and further filtered to remove all those that were also identified in the IgG IPs without being enriched in the TOP1 IPs by at least twofold based on their % coverage values. Keratins and trypsin which are introduced during the IP-MS procedure were deleted from the results. STRING network and Metascape GO analyses were performed on the list of factors identified following these criteria in both biological replicates of control and RNase conditions.

Acknowledgement: This paper is coauthored with Rahnamoun, Homa. The thesis author was the primary author of this paper.

Supplementary Table 1. Oligonucleotide sequences for amplification of genomic regions corresponding to various RNA species used for *in vitro* RNA synthesis

Name	**Primer Sequence**	**RNA length**
NORAD F	CCGGATCCTAATACGACTCACTATAGAGTTCCGGTCCGGCAGAGAT	800 bp
NORAD R	TTGCGGCCGCTTGGGGTGGAGTTGAGAGC	
45S rRNA F	CCGGTACCTAATACGACTCACTATAGGAAGCCAGAGGAAACTCT	250 bp
45S rRNA R	TTCTCGAGTACCCATTTAAAGTTTGAGAATAG	
MMP9 eRNA F	CCGGTACCTAATACGACTCACTATAGGCTGGCATATATGATGACT	260 bp
MMP9 eRNA R	TTCTCGAGGCTGGCATATCAGACAG	
CCL2 eRNA F	CCGGTACCTAATACGACTCACTATAGCTTTATCTATGAGTTGATAG	286 bp
CCL2 eRNA R	TTCTCGAGAGCTTTGGAAGTTCCCAG	

Supplementary Table 2. Oligonucleotide sequences for RT-PCR analysis of gene expression

Name	**Sequence**
GAPDH F	ATTTGGTCGTATTGGGCGCCTG
GAPDH R	AGCCTTGACGGTGCCATGGAATTT
NORAD F	CTCTGCTGTGGCTGCCC
NORAD R	GGGTGGGAAAGAGAGGTTCG
18S rRNA F	GCTTAATTTGACTCAACACGGGA
18S rRNA R	AGCTATCAATCTGTCAATCCTGTC
snoRNA 118 F	GGTGGGATAATCCTTACCTGTTC
snoRNA 118 R	CCTGATTACGCAGAGACGTTAAT
CSF2 eRNA F	CTGAAGCTGTGAGCAGAGAAA
CSF2 eRNA R	CCAAGTAGCAGGAAGAGTGATG
CSF2 mRNA F	GTCTCCTGAACCTGAGTAGAGA
CSF2 mRNA R	GGTCAAACATTTCTGAGATGACTTC
45S rRNA F	CACGGACAGGATTGACAGATT
45S rRNA R	GCCAGAGTCTCGTTCGTTATC

Supplementary Table 3. Oligonucleotide sequences for ASO transfections

Name	**Sequence**
CCL2 eRNA ASO	/52MOErA/*/i2MOErG/*+A*T*A*C*T*G*G*G*C*C*C*+G*+G*/32MOErA/
Control (NC1)	/52MOErG/*/i2MOErT/*+T* A*A*T* C*G*C* G*T*A* T*A*A* T*A*+C* +G*/32MOErC/

References

1. Liu, L. F.; Wang, J. C., Supercoiling of the DNA template during transcription. *Proc Natl Acad Sci U S A* **1987,** *84* (20), 7024-7.

2. Durand-Dubief, M.; Persson, J.; Norman, U.; Hartsuiker, E.; Ekwall, K., Topoisomerase I regulates open chromatin and controls gene expression in vivo. *EMBO J* **2010,** *29* (13), 2126-34.

3. Durand-Dubief, M.; Svensson, J. P.; Persson, J.; Ekwall, K., Topoisomerases, chromatin and transcription termination. *Transcription* **2011,** *2* (2), 66-70.

4. Pommier, Y.; Sun, Y.; Huang, S. N.; Nitiss, J. L., Roles of eukaryotic topoisomerases in transcription, replication and genomic stability. *Nat Rev Mol Cell Biol* **2016,** *17* (11), 703-721.

5. Ma, J.; Bai, L.; Wang, M. D., Transcription under torsion. *Science* **2013,** *340* (6140), 1580-3.

6. Roca, J., Transcriptional inhibition by DNA torsional stress. *Transcription* **2011,** *2* (2), 82-85.

7. Aguilera, A.; García-Muse, T., R loops: from transcription byproducts to threats to genome stability. *Mol Cell* **2012,** *46* (2), 115-24.

8. Kouzine, F.; Gupta, A.; Baranello, L.; Wojtowicz, D.; Ben-Aissa, K.; Liu, J.; Przytycka, T. M.; Levens, D., Transcription-dependent dynamic supercoiling is a short-range genomic force. *Nat Struct Mol Biol* **2013,** *20* (3), 396-403.

9. Champoux, J. J., DNA topoisomerases: structure, function, and mechanism. *Annu Rev Biochem* **2001,** *70*, 369-413.

10. Pommier, Y., Drugging topoisomerases: lessons and challenges. *ACS Chem Biol* **2013,** *8* (1), 82-95.

11. Muller, M. T.; Pfund, W. P.; Mehta, V. B.; Trask, D. K., Eukaryotic type I topoisomerase is enriched in the nucleolus and catalytically active on ribosomal DNA. *EMBO J* **1985,** *4* (5), 1237-43.

12. Zhang, H.; Wang, J. C.; Liu, L. F., Involvement of DNA topoisomerase I in transcription of human ribosomal RNA genes. *Proc Natl Acad Sci U S A* **1988,** *85* (4), 1060-4.

13. Mao, Y.; Mehl, I. R.; Muller, M. T., Subnuclear distribution of topoisomerase I is linked to ongoing transcription and p53 status. *Proc Natl Acad Sci U S A* **2002,** *99* (3), 1235-40.

14. Brill, S. J.; DiNardo, S.; Voelkel-Meiman, K.; Sternglanz, R., Need for DNA topoisomerase activity as a swivel for DNA replication for transcription of ribosomal RNA. *Nature* **1987,** *326* (6111), 414-6.

15. Rose, K. M.; Szopa, J.; Han, F. S.; Cheng, Y. C.; Richter, A.; Scheer, U., Association of DNA topoisomerase I and RNA polymerase I: a possible role for topoisomerase I in ribosomal gene transcription. *Chromosoma* **1988,** *96* (6), 411-6.

16. Christensen, M. O.; Barthelmes, H. U.; Boege, F.; Mielke, C., The N-terminal domain anchors human topoisomerase I at fibrillar centers of nucleoli and nucleolar organizer regions of mitotic chromosomes. *J Biol Chem* **2002,** *277* (39), 35932-8.

17. El Hage, A.; French, S. L.; Beyer, A. L.; Tollervey, D., Loss of Topoisomerase I leads to R-loop-mediated transcriptional blocks during ribosomal RNA synthesis. *Genes Dev* **2010,** *24* (14), 1546-58.

18. Tafforeau, L.; Zorbas, C.; Langhendries, J. L.; Mullineux, S. T.; Stamatopoulou, V.; Mullier, R.; Wacheul, L.; Lafontaine, D. L., The complexity of human ribosome biogenesis revealed by systematic nucleolar screening of Pre-rRNA processing factors. *Mol Cell* **2013,** *51* (4), 539-51.

19. Shen, W.; Sun, H.; De Hoyos, C. L.; Bailey, J. K.; Liang, X. H.; Crooke, S. T., Dynamic nucleoplasmic and nucleolar localization of mammalian RNase H1 in response to RNAP I transcriptional R-loops. *Nucleic Acids Res* **2017,** *45* (18), 10672-10692.

20. Shykind, B. M.; Kim, J.; Stewart, L.; Champoux, J. J.; Sharp, P. A., Topoisomerase I enhances TFIID-TFIIA complex assembly during activation of transcription. *Genes Dev* **1997,** *11* (3), 397-407.

21. Kretzschmar, M.; Meisterernst, M.; Roeder, R. G., Identification of human DNA topoisomerase I as a cofactor for activator-dependent transcription by RNA polymerase II. *Proc Natl Acad Sci U S A* **1993,** *90* (24), 11508-12.

22. Baranello, L.; Wojtowicz, D.; Cui, K.; Devaiah, B. N.; Chung, H. J.; Chan-Salis, K. Y.; Guha, R.; Wilson, K.; Zhang, X.; Zhang, H.; Piotrowski, J.; Thomas, C. J.; Singer, D. S.; Pugh, B. F.; Pommier, Y.; Przytycka, T. M.; Kouzine, F.; Lewis, B. A.; Zhao, K.; Levens, D., RNA Polymerase II Regulates Topoisomerase 1 Activity to Favor Efficient Transcription. *Cell* **2016,** *165* (2), 357-71.

23. Puc, J.; Kozbial, P.; Li, W.; Tan, Y.; Liu, Z.; Suter, T.; Ohgi, K. A.; Zhang, J.; Aggarwal, A. K.; Rosenfeld, M. G., Ligand-dependent enhancer activation regulated by topoisomerase-I activity. *Cell* **2015,** *160* (3), 367-80.

24. Bansal, K.; Yoshida, H.; Benoist, C.; Mathis, D., The transcriptional regulator Aire binds to and activates super-enhancers. *Nat Immunol* **2017,** *18* (3), 263-273.

25. Christensen, M. O.; Barthelmes, H. U.; Feineis, S.; Knudsen, B. R.; Andersen, A. H.; Boege, F.; Mielke, C., Changes in mobility account for camptothecin-induced subnuclear relocation of topoisomerase I. *J Biol Chem* **2002,** *277* (18), 15661-5.

26. Buckwalter, C. A.; Lin, A. H.; Tanizawa, A.; Pommier, Y. G.; Cheng, Y. C.; Kaufmann, S. H., RNA synthesis inhibitors alter the subnuclear distribution of DNA topoisomerase I. *Cancer Res* **1996,** *56* (7), 1674-81.

27. Mo, Y. Y.; Yu, Y.; Shen, Z.; Beck, W. T., Nucleolar delocalization of human topoisomerase I in response to topotecan correlates with sumoylation of the protein. *J Biol Chem* **2002,** *277* (4), 2958-64.

28. Mao, Y.; Sun, M.; Desai, S. D.; Liu, L. F., SUMO-1 conjugation to topoisomerase I: A possible repair response to topoisomerase-mediated DNA damage. *Proc Natl Acad Sci U S A* **2000,** *97* (8), 4046-51.

29. Rallabhandi, P.; Hashimoto, K.; Mo, Y. Y.; Beck, W. T.; Moitra, P. K.; D'Arpa, P., Sumoylation of topoisomerase I is involved in its partitioning between nucleoli and nucleoplasm and its clearing from nucleoli in response to camptothecin. *J Biol Chem* **2002,** *277* (42), 40020-6.

30. Karayan, L.; Riou, J. F.; Séité, P.; Migeon, J.; Cantereau, A.; Larsen, C. J., Human ARF protein interacts with topoisomerase I and stimulates its activity. *Oncogene* **2001,** *20* (7), 836-48.

31. Bowen, C.; Stuart, A.; Ju, J. H.; Tuan, J.; Blonder, J.; Conrads, T. P.; Veenstra, T. D.; Gelmann, E. P., NKX3.1 homeodomain protein binds to topoisomerase I and enhances its activity. *Cancer Res* **2007,** *67* (2), 455-64.

32. Mao, Y.; Okada, S.; Chang, L. S.; Muller, M. T., p53 dependence of topoisomerase I recruitment in vivo. *Cancer Res* **2000,** *60* (16), 4538-43.

33. Goswami, A.; Qiu, S.; Dexheimer, T. S.; Ranganathan, P.; Burikhanov, R.; Pommier, Y.; Rangnekar, V. M., Par-4 binds to topoisomerase 1 and attenuates its DNA relaxation activity. *Cancer Res* **2008,** *68* (15), 6190-8.

34. Li, M.; Pokharel, S.; Wang, J. T.; Xu, X.; Liu, Y., RECQ5-dependent SUMOylation of DNA topoisomerase I prevents transcription-associated genome instability. *Nat Commun* **2015,** *6*, 6720.

35. Cassiday, L. A.; Maher, L. J., Having it both ways: transcription factors that bind DNA and RNA. *Nucleic Acids Res* **2002,** *30* (19), 4118-26.

36. Sigova, A. A.; Abraham, B. J.; Ji, X.; Molinie, B.; Hannett, N. M.; Guo, Y. E.; Jangi, M.; Giallourakis, C. C.; Sharp, P. A.; Young, R. A., Transcription factor trapping by RNA in gene regulatory elements. *Science* **2015,** *350* (6263), 978-81.

37. Castello, A.; Fischer, B.; Eichelbaum, K.; Horos, R.; Beckmann, B. M.; Strein, C.; Davey, N. E.; Humphreys, D. T.; Preiss, T.; Steinmetz, L. M.; Krijgsveld, J.; Hentze, M. W., Insights into RNA biology from an atlas of mammalian mRNA-binding proteins. *Cell* **2012,** *149* (6), 1393-406.

38. Baltz, A. G.; Munschauer, M.; Schwanhäusser, B.; Vasile, A.; Murakawa, Y.; Schueler, M.; Youngs, N.; Penfold-Brown, D.; Drew, K.; Milek, M.; Wyler, E.; Bonneau, R.; Selbach, M.; Dieterich, C.; Landthaler, M., The mRNA-bound proteome and its global occupancy profile on protein-coding transcripts. *Mol Cell* **2012,** *46* (5), 674-90.

39. He, C.; Sidoli, S.; Warneford-Thomson, R.; Tatomer, D. C.; Wilusz, J. E.; Garcia, B. A.; Bonasio, R., High-Resolution Mapping of RNA-Binding Regions in the Nuclear Proteome of Embryonic Stem Cells. *Mol Cell* **2016,** *64* (2), 416-430.

40. Munschauer, M.; Nguyen, C. T.; Sirokman, K.; Hartigan, C. R.; Hogstrom, L.; Engreitz, J. M.; Ulirsch, J. C.; Fulco, C. P.; Subramanian, V.; Chen, J.; Schenone, M.; Guttman, M.; Carr, S. A.; Lander, E. S., The NORAD lncRNA assembles a topoisomerase complex critical for genome stability. *Nature* **2018,** *561* (7721), 132-136.

41. Caudron-Herger, M.; Rusin, S. F.; Adamo, M. E.; Seiler, J.; Schmid, V. K.; Barreau, E.; Kettenbach, A. N.; Diederichs, S., R-DeeP: Proteome-wide and Quantitative Identification of RNA-Dependent Proteins by Density Gradient Ultracentrifugation. *Mol Cell* **2019,** *75* (1), 184-199.e10.

42. Lanza, A.; Tornaletti, S.; Rodolfo, C.; Scanavini, M. C.; Pedrini, A. M., Human DNA topoisomerase I-mediated cleavages stimulated by ultraviolet light-induced DNA damage. *J Biol Chem* **1996,** *271* (12), 6978-86.

43. Bendak, K.; Loughlin, F. E.; Cheung, V.; O'Connell, M. R.; Crossley, M.; Mackay, J. P., A rapid method for assessing the RNA-binding potential of a protein. *Nucleic Acids Res* **2012,** *40* (14), e105.

44. Rahnamoun, H.; Lu, H.; Duttke, S. H.; Benner, C.; Glass, C. K.; Lauberth, S. M., Mutant p53 shapes the enhancer landscape of cancer cells in response to chronic immune signaling. *Nat Commun* **2017,** *8* (1), 754.

45. Hayano, T.; Yanagida, M.; Yamauchi, Y.; Shinkawa, T.; Isobe, T.; Takahashi, N., Proteomic analysis of human Nop56p-associated pre-ribosomal ribonucleoprotein complexes. Possible link between Nop56p and the nucleolar protein treacle responsible for Treacher Collins syndrome. *J Biol Chem* **2003,** *278* (36), 34309-19.

46. Liu, Z.; Zhou, Z.; Chen, G.; Bao, S., A putative transcriptional elongation factor hIws1 is essential for mammalian cell proliferation. *Biochem Biophys Res Commun* **2007,** *353* (1), 47-53.

47. Lindström, M. S., NPM1/B23: A Multifunctional Chaperone in Ribosome Biogenesis and Chromatin Remodeling. *Biochem Res Int* **2011,** *2011*, 195209.

48. Hochstatter, J.; Hölzel, M.; Rohrmoser, M.; Schermelleh, L.; Leonhardt, H.; Keough, R.; Gonda, T. J.; Imhof, A.; Eick, D.; Längst, G.; Németh, A., Myb-binding protein 1a (Mybbp1a) regulates levels and processing of pre-ribosomal RNA. *J Biol Chem* **2012,** *287* (29), 24365-77.

49. Li, X.; Wang, W.; Wang, J.; Malovannaya, A.; Xi, Y.; Li, W.; Guerra, R.; Hawke, D. H.; Qin, J.; Chen, J., Proteomic analyses reveal distinct chromatin-associated and soluble transcription factor complexes. *Mol Syst Biol* **2015,** *11* (1), 775.

50. Liccardi, G.; Hartley, J. A.; Hochhauser, D., Importance of EGFR/ERCC1 interaction following radiation-induced DNA damage. *Clin Cancer Res* **2014,** *20* (13), 3496-506.

51. Kroeger, P. E.; Rowe, T. C., Interaction of topoisomerase 1 with the transcribed region of the Drosophila HSP 70 heat shock gene. *Nucleic Acids Res* **1989,** *17* (21), 8495-509.

52. Ciavarra, R. P.; Goldman, C.; Wen, K. K.; Tedeschi, B.; Castora, F. J., Heat stress induces hsc70/nuclear topoisomerase I complex formation in vivo: evidence for hsc70-mediated, ATP-independent reactivation in vitro. *Proc Natl Acad Sci U S A* **1994,** *91* (5), 1751-5.

53. Mukherjee, C.; Tripathi, V.; Manolika, E. M.; Heijink, A. M.; Ricci, G.; Merzouk, S.; de Boer, H. R.; Demmers, J.; van Vugt, M. A. T. M.; Ray Chaudhuri, A., RIF1 promotes replication fork protection and efficient restart to maintain genome stability. *Nat Commun* **2019,** *10* (1), 3287.

54. Lubas, M.; Andersen, P. R.; Schein, A.; Dziembowski, A.; Kudla, G.; Jensen, T. H., The human nuclear exosome targeting complex is loaded onto newly synthesized RNA to direct early ribonucleolysis. *Cell Rep* **2015,** *10* (2), 178-92.

55. Pefanis, E.; Wang, J.; Rothschild, G.; Lim, J.; Kazadi, D.; Sun, J.; Federation, A.; Chao, J.; Elliott, O.; Liu, Z. P.; Economides, A. N.; Bradner, J. E.; Rabadan, R.; Basu, U., RNA exosome-regulated long non-coding RNA transcription controls super-enhancer activity. *Cell* **2015,** *161* (4), 774-89.

56. Raj, A.; van Oudenaarden, A., Nature, nurture, or chance: stochastic gene expression and its consequences. *Cell* **2008,** *135* (2), 216-26.

57. Nicolas, D.; Phillips, N. E.; Naef, F., What shapes eukaryotic transcriptional bursting? *Mol Biosyst* **2017,** *13* (7), 1280-1290.

58. Coulon, A.; Chow, C. C.; Singer, R. H.; Larson, D. R., Eukaryotic transcriptional dynamics: from single molecules to cell populations. *Nat Rev Genet* **2013,** *14* (8), 572-84.

59. Molina, N.; Suter, D. M.; Cannavo, R.; Zoller, B.; Gotic, I.; Naef, F., Stimulus-induced modulation of transcriptional bursting in a single mammalian gene. *Proc Natl Acad Sci U S A* **2013,** *110* (51), 20563-8.

60. Brogna, S.; Sato, T. A.; Rosbash, M., Ribosome components are associated with sites of transcription. *Mol Cell* **2002,** *10* (4), 93-104.

61. Dumbar, T. S.; Gentry, G. A.; Olson, M. O., Interaction of nucleolar phosphoprotein B23 with nucleic acids. *Biochemistry* **1989,** *28* (24), 9495-501.

62. Herrera, J. E.; Savkur, R.; Olson, M. O., The ribonuclease activity of nucleolar protein B23. *Nucleic Acids Res* **1995,** *23* (19), 3974-9.

63. Mitrea, D. M.; Cika, J. A.; Guy, C. S.; Ban, D.; Banerjee, P. R.; Stanley, C. B.; Nourse, A.; Deniz, A. A.; Kriwacki, R. W., Nucleophosmin integrates within the nucleolus via multi-modal interactions with proteins displaying R-rich linear motifs and rRNA. *Elife* **2016,** *5*.

64. Feric, M.; Vaidya, N.; Harmon, T. S.; Mitrea, D. M.; Zhu, L.; Richardson, T. M.; Kriwacki, R. W.; Pappu, R. V.; Brangwynne, C. P., Coexisting Liquid Phases Underlie Nucleolar Subcompartments. *Cell* **2016,** *165* (7), 1686-1697.

65. Banani, S. F.; Lee, H. O.; Hyman, A. A.; Rosen, M. K., Biomolecular condensates: organizers of cellular biochemistry. *Nat Rev Mol Cell Biol* **2017,** *18* (5), 285-298.

66. Mo, Y. Y.; Wang, C.; Beck, W. T., A novel nuclear localization signal in human DNA topoisomerase I. *J Biol Chem* **2000,** *275* (52), 41107-13.

67. D'Arpa, P.; Machlin, P. S.; Ratrie, H.; Rothfield, N. F.; Cleveland, D. W.; Earnshaw, W. C., cDNA cloning of human DNA topoisomerase I: catalytic activity of a 67.7-kDa carboxyl-terminal fragment. *Proc Natl Acad Sci U S A* **1988,** *85* (8), 2543-7.

68. Stewart, L.; Ireton, G. C.; Champoux, J. J., The domain organization of human topoisomerase I. *J Biol Chem* **1996,** *271* (13), 7602-8.

69. Alsner, J.; Svejstrup, J. Q.; Kjeldsen, E.; Sørensen, B. S.; Westergaard, O., Identification of an N-terminal domain of eukaryotic DNA topoisomerase I dispensable for catalytic activity but essential for in vivo function. *J Biol Chem* **1992,** *267* (18), 12408-11.

70. Rahnamoun, H.; Lee, J.; Sun, Z.; Lu, H.; Ramsey, K. M.; Komives, E. A.; Lauberth, S. M., RNAs interact with BRD4 to promote enhanced chromatin engagement and transcription activation. *Nat Struct Mol Biol* **2018,** *25* (8), 687-697.

71. Fei, J.; Ishii, H.; Hoeksema, M. A.; Meitinger, F.; Kassavetis, G. A.; Glass, C. K.; Ren, B.; Kadonaga, J. T., NDF, a nucleosome-destabilizing factor that facilitates transcription through nucleosomes. *Genes Dev* **2018,** *32* (9-10), 682-694.

72. McCormack, A. L.; Schieltz, D. M.; Goode, B.; Yang, S.; Barnes, G.; Drubin, D.; Yates, J. R., Direct analysis and identification of proteins in mixtures by LC/MS/MS and database searching at the low-femtomole level. *Anal Chem* **1997,** *69* (4), 767-76.
73. Guttman, M.; Betts, G. N.; Barnes, H.; Ghassemian, M.; van der Geer, P.; Komives, E. A., Interactions of the NPXY microdomains of the low density lipoprotein receptor-related protein 1. *Proteomics* **2009,** *9* (22), 5016-28.